ARCHIVES OF ACOUSTICS
27, 3, 217–228 (2002)

TEMPERATURE DISTRIBUTION FORMULAE APPLICATIONS IN PHOTOACOUSTICS

M. MALIŃSKI

Department of Electronics – Technical University of Koszalin
17 Partyzantów St, 75-411 Koszalin Poland.

This paper presents the new formula for the distribution of a periodical component of the temperature in the samples excited by the periodically modulated beam of light. It was shown that this formula enables the piezoelectric photoacoustic spectra analysis and interpretations. The influence of the backing material on the temperature distributions in the sample and piezoelectric photoacoustic spectra was presented and analyzed.

1. Introduction

The temperature formulae presented in the paper describe spatial distributions of periodical contributions of the temperature alongside the thickness of the sample shaped in the form of a parallel plate placed on the thermally thick backing material. This periodical temperature contribution is the result of the periodical generation of the heat flux in the sample illuminated by the chopped beam of light. The example spatial distributions of the instantaneous temperature as well as the amplitude and the phase of the temperature are presented. They are especially important from the point of view of their influence on the photoacoustic spectral characteristics of semiconductor materials observed both in the microphone and piezoelectric detection used in the field of photoacoustic spectroscopy. Constantly increasing amount of the experimental data of the piezoelectric photoacoustic spectra of both n and p type Si crystals [1, 2], AIII-BVI materials for solar cells applications [3], AIII-BV [4, 5] and AII-BVI [6, 7, 8] caused a necessity of developing interpretation tools especially for the piezoelectric photoacoustic spectra.

2. Description of the model

The material of a sample and the backing is characterised by the following parameters: λ — thermal conductivity, α – thermal diffusivity, μ – thermal diffusion length, e_s and e_b thermal effusivities of the sample and the backing respectively, R – thermal reflection coefficient between the sample and the backing, l – thickness of the sample, β – optical absorption coefficient. The notations used in the formula are: $\sigma(f) = (1+i)/\mu$, $\mu = (\alpha/\pi \cdot f)^{1/2}$

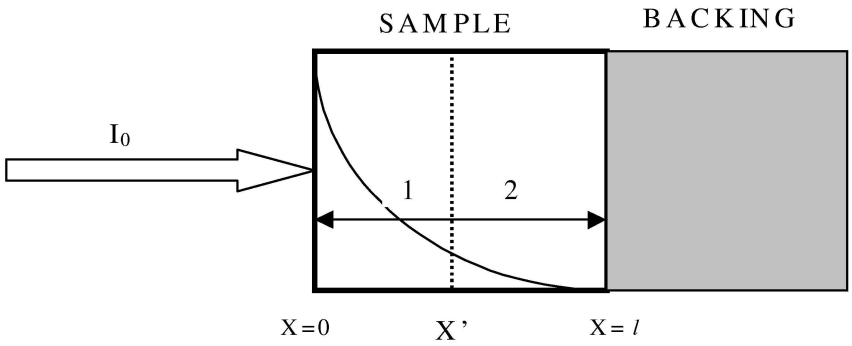

Fig. 1. The schematic diagram of the theoretical situation considered in the paper — The configuration: beam of light-sample-backing.

Theoretical considerations performed with the use of the thermal wave interference method and the configuration of the objects presented in Fig. 1 lead to the formula for the spatial temperature distribution.

The formulae presented in this paper were derived on the basis of the thermal wave interference method proposed by A. ROSENCWAIG [9] and BENETT and PATTY [10]. In these papers the formulae for the temperature of the front side of the samples were derived. They were necessary for the interpretation of the experimental results obtained with the microphone detection measuring method. This method of detection is sensitive to the temperature of the front (or rear) side of the sample. The analysis of the piezoelectric signals however brought about the necessity of the derivation of the temperature distribution formula for the samples placed on different backing materials as the value of the piezoelectric signal depends on the temperature distribution in the sample. The derivation of the spatial temperature distribution formula and the analysis of the influence of the temperature distribution in the sample on the piezoelectric photoacoustic spectra are the subject of the presented paper. The influence of the thermal parameters of the backing materials on the piezoelectric spectra has not been analyzed in literature in detail so far.

The thermal wave interference method, used in this paper for the purpose of the derivation of the temperature distribution in the sample, was applied successfully in the metrology of thermal parameters of different materials [11-15] and in the analysis of photoacoustic microphone detected spectra [16-18]. This thermal wave interference method is based on some basic assumptions:

a) The temperature originally generated in the point described by the x coordinate is given by the formula:

$$T(x,t) = \beta \cdot Io \cdot (\exp(-\beta \cdot x)/\lambda \cdot \sigma) \cdot \exp(i \cdot \omega \cdot t).$$

b) Temperature at the distance d from the point of its generation is described by the formula:

$$T(d) = T(x) \cdot \exp(-\sigma \cdot d).$$

c) The thermal reflection coefficient R between the sample and the backing is determined by the thermal effusivities of the sample and the backing as:

$$R = (e_s - e_b)/(e_s + e_b).$$

The boundary conditions assumed in this paper are the following.

The thermal reflection coefficients for the front $(x' = 0)$ and rear $(x' = l)$ sides of the sample are 1 and R respectively. The diameter of the sample is big enough to neglect the reflections from the top and bottom sides of the sample (see Fig. 1). The diameter of the spot of light is bigger than the thickness of the sample. The steady-state conditions are fulfilled in that sense that the amplitude and phase of the temperature do not depend on time.

The distribution of the intensity of light in the sample is described by the formula:

$$I(x) = I_0 \cdot \exp(-\beta \cdot x). \tag{2.1}$$

Due to the absorption of the in intensity modulated beam of light the corresponding distribution of the periodical temperature originally generated in the sample appears $T(x,t)$ (see point a). Next, generated this way, plane thermal waves travel to the left and to the right in the sample. Their amplitude and phase change as a function of the propagation distance (see point b). These thermal waves reflect repeatedly from the front and rear sides of the sample (see point c) and interfere. Let x is the place of the generation of the original thermal wave. $T(x', x)$ are the thermal wave components that give the resulting temperature $T(x')$ at the point x'. The final temperature distribution is the result of the integration of all contributions $T(x', x)$ from all places in a sample $0 < x < l$.

$$T(x') = \int_0^l T(x', x)\, dx. \tag{2.2}$$

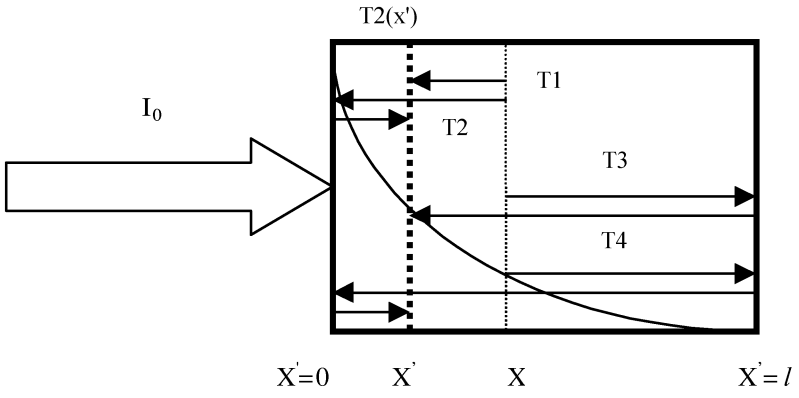

Fig. 2. Schematic presentation of the four thermal wave contributions to the temperature $T_2(x')$ – at the point x'. X-notes the place of the original generation of the temperature. An assumption $x > x'$.

The temperature $T_2(x')$ for $R = 1$ can be expressed as:

$$T_2(x') = \int_{x'}^{l} (T1(x) + T2(x) + T3(x) + T4(x))\, dx, \tag{2.3}$$

$$T_2(x') = \frac{\beta \cdot I_0}{\lambda \cdot \sigma \cdot (1 - \exp(-2 \cdot \sigma \cdot l))} \cdot \int_{x'}^{l} \Big[\exp(-\sigma \cdot (x - x')) + \exp(-\sigma \cdot (x + x')) + \exp(-\sigma \cdot (2 \cdot l - x - x')) + \exp(-\sigma \cdot (2 \cdot l - x + x')) \Big] \cdot \exp(-\beta \cdot x)\, dx. \tag{2.4}$$

On the other hand the total contributions to the temperature at the point x' coming from the points of the original heat generation whose coordinates fulfil the condition $x < x'$ are described by the function (2.5).

$$T_1(x') = \frac{\beta \cdot I_0}{\lambda \cdot \sigma \cdot (1 - \exp(-2 \cdot \sigma \cdot l))} \cdot \int_{0}^{x'} \Big[\exp(-\sigma \cdot (x' - x)) + \exp(-\sigma \cdot (2 \cdot l - x - x')) + \exp(-\sigma \cdot (x + x')) + \exp(-\sigma \cdot (2 \cdot l + x - x')) \Big] \cdot \exp(-\beta \cdot x)\, dx. \tag{2.5}$$

The total temperature at the point characterised by the x' coordinate is thus determined as:

$$T(x', t) = T(x') \cdot \exp(i \cdot \omega \cdot t) \qquad \text{where} \quad T(x') = (T_1(x') + T_2(x'))/2. \tag{2.6}$$

After the computations the following final formula was obtained:

$$T(x') = \frac{\beta \cdot I_0}{2 \cdot \lambda \cdot \sigma \cdot (1 - \exp(-2 \cdot \sigma \cdot l))} \cdot [M(x') + N(x')], \tag{2.7}$$

where $M(x')$ and $N(x')$ are given by the following formulae:

$$M(x') = \frac{[\exp(\sigma \cdot x') + \exp(-\sigma \cdot x')] \cdot [\exp((-\sigma - \beta) \cdot x') - \exp((-\sigma - \beta) \cdot l)]}{\beta + \sigma} + \frac{\exp(-2 \cdot \sigma \cdot l) \cdot [\exp(\sigma \cdot x') + \exp(-\sigma \cdot x')] \cdot [\exp((\sigma - \beta) \cdot x') - \exp((\sigma - \beta) \cdot l)]}{\beta - \sigma} \tag{2.8}$$

$$N(x') = \frac{[\exp(-\sigma \cdot x') + \exp(-2 \cdot \sigma \cdot l + \sigma \cdot x')] \cdot [1 - \exp((-\sigma - \beta) \cdot x')]}{\beta + \sigma} + \frac{[\exp(-\sigma \cdot x') + \exp(-2 \cdot \sigma \cdot l + \sigma \cdot x')] \cdot [1 - \exp((\sigma - \beta) \cdot x')]}{\beta - \sigma}. \tag{2.9}$$

This temperature distribution formula (2.7) – (2.9) is limited to the samples placed on a thermally insulating backing material such as for example air backing. This temperature distribution formula derived for $R = 1$ is presented here because this kind of backing material is recommended in the piezo photoacoustic experiments.

The temperature distribution formula for much more general case for the thermal reflection coefficient R between the backing and the sample was next derived, following the steps presented for $R = 1$, and is presented below.

$$T_2(x') = \frac{\beta \cdot I_0}{\lambda \cdot \sigma \cdot (1 - R \cdot \exp(-2 \cdot \sigma \cdot l))} \cdot \int_{x'}^{l} \Big[\exp(-\sigma \cdot (x - x')) + \exp(-\sigma \cdot (x + x'))$$
$$+ R \cdot \exp(-\sigma \cdot (2 \cdot l - x - x')) + R \cdot \exp(-\sigma \cdot (2 \cdot l - x + x')) \Big] \cdot \exp(-\beta \cdot x)\, dx. \tag{2.10}$$

$$T_1(x') = \frac{\beta \cdot I_0}{\lambda \cdot \sigma \cdot (1 - R \cdot \exp(-2 \cdot \sigma \cdot l))} \cdot \int_{0}^{x'} \Big[\exp(-\sigma \cdot (x' - x)) + R \cdot \exp(-\sigma \cdot (2 \cdot l - x - x'))$$
$$+ \exp(-\sigma \cdot (x + x')) + R \cdot \exp(-\sigma \cdot (2 \cdot l + x - x')) \Big] \cdot \exp(-\beta \cdot x)\, dx. \tag{2.11}$$

$$T(x', t) = T(x') \cdot \exp(i \cdot \omega \cdot t) \qquad T(x') = (T_1(x') + T_2(x'))/2. \tag{2.12}$$

$$T(x') = \frac{\beta \cdot I_0}{2 \cdot \lambda \cdot \sigma \cdot (1 - R \cdot \exp(-2 \cdot \sigma \cdot l))} \cdot [M(x') + N(x')]\,. \tag{2.13}$$

$$M(x') = \frac{[\exp(\sigma \cdot x') + \exp(-\sigma \cdot x')] \cdot [\exp((-\sigma - \beta) \cdot x') - \exp((-\sigma - \beta) \cdot l)]}{\beta + \sigma}$$
$$+ \frac{R \cdot \exp(-2 \cdot \sigma \cdot l) \cdot [\exp(\sigma \cdot x') + \exp(-\sigma \cdot x')][\exp((\sigma - \beta) \cdot x') - \exp((\sigma - \beta) \cdot l)]}{\beta - \sigma}. \tag{2.14}$$

$$N(x') = \frac{[\exp(-\sigma \cdot x') + R \cdot \exp(-2 \cdot \sigma \cdot l + \sigma \cdot x')] \cdot [1 - \exp((-\sigma - \beta) \cdot x')]}{\beta + \sigma}$$
$$+ \frac{[\exp(-\sigma \cdot x') + R \cdot \exp(-2 \cdot \sigma \cdot l + \sigma \cdot x')] \cdot [1 - \exp((\sigma - \beta) \cdot x')]}{\beta - \sigma}\,. \tag{2.15}$$

3. Specific temperature distributions

The temperature distribution $T(x')$ (2.13) – (2.15) is in fact depending on several material and experimental parameters, introduced earlier, so it can be written as:

$$T(x') = T(x', \alpha, R, \beta, l, f). \tag{3.1}$$

This temperature distribution formula derived above given by expressions (2.13) – (2.15) was next verified and compared with well known temperature characteristics at some characteristic points of the sample and experimental configurations i.e. at the front and rear sides of the sample. In the mathematical sense they are special cases of the general formula presented in this paper. The comparison comprised the following special cases presented in Fig. 3.

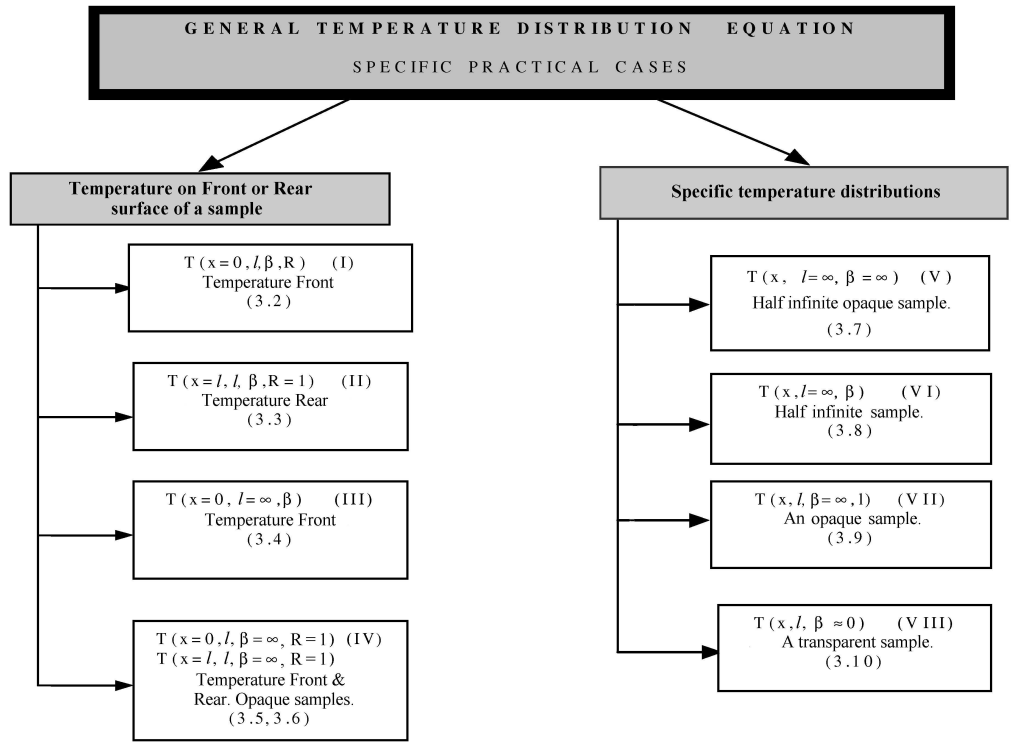

Fig. 3. Special characteristic cases of the temperature distribution formula.

Example specific cases of the general temperature distribution formula (2.13) – (2.15)

A) Temperature on front and rear surface of a sample

Ad I. Temperature of the front surface of the sample. $T(x = 0, l, \beta, R)$ [10]

$$T_F = \frac{\beta \cdot I_0}{\lambda \cdot \sigma} \cdot \left[\frac{\dfrac{1 - \exp(-(\beta + \sigma) \cdot l)}{\sigma + \beta} + \dfrac{R \cdot \exp(-2 \cdot \sigma \cdot l)(1 - \exp(-(\beta - \sigma) \cdot l))}{\beta - \sigma}}{1 - R \cdot \exp(-2 \cdot \sigma \cdot l)} \right]. \quad (3.2)$$

Ad II. Temperature of the rear surface of the sample $T(x = l, l, \beta, R = 1)$

$$T_R = \frac{\beta \cdot I_0}{\lambda \cdot \sigma} \cdot \left[\frac{\dfrac{\exp(-\sigma \cdot l) \cdot (1 - \exp(-(\sigma + \beta) \cdot l))}{\sigma + \beta}}{1 - \exp(-2 \cdot \sigma \cdot l)} + \frac{\dfrac{\exp(-\sigma \cdot l) \cdot (1 - \exp((\sigma - \beta) \cdot l))}{\beta - \sigma}}{1 - \exp(-2 \cdot \sigma \cdot l)} \right]. \quad (3.3)$$

Ad III. Temperature of the front surface of a half-infinite sample $T(x = 0,\ l = \infty, \beta)$ [16]

$$T^*(0) = \frac{\beta \cdot I_0}{\lambda \cdot \sigma \cdot (\beta + \sigma)}\,. \tag{3.4}$$

Ad IV. Temperature of a front surface of an opaque sample thermally thin $T(x = 0, l, \beta = \infty, R = 1)$ [12].

$$T^*(0) = \frac{I_0}{\lambda \cdot \sigma} \cdot \frac{\cosh(\sigma \cdot l)}{\sinh(\sigma \cdot l)}\,. \tag{3.5}$$

Temperature of the rear surface of an opaque sample thermally thin $T(x = l, l, \beta = \infty, R = 1)$ [12].

$$T^*(l) = \frac{I_0}{\lambda \cdot \sigma} \cdot \frac{1}{\sinh(\sigma \cdot l)}\,. \tag{3.6}$$

B) Other specific temperature distributions.

Ad. V. Temperature distribution in an opaque half infinite sample $T(x, l = \infty, \beta = \infty)$

$$T^*(X') = \frac{I_0}{\lambda \cdot \sigma} \cdot \exp(-\sigma \cdot X'). \tag{3.7}$$

Ad. VI. Temperature distribution in a half infinite sample $T(x, l = \infty, \beta)$

$$T^*(X') = \frac{\beta \cdot I_0}{\lambda \cdot \sigma} \cdot \left[\frac{\exp(-\sigma \cdot X') + \exp(-\beta \cdot X')}{\beta + \sigma} + \frac{\exp(-\sigma \cdot X') - \exp(-\beta \cdot X')}{\beta - \sigma}\right]. \tag{3.8}$$

Ad. VII. Temperature distribution in an opaque sample. $T(x, l, \beta = \infty, R = 1)$.

$$T^*(X') = \frac{I_0}{\lambda \cdot \sigma} \cdot \left[\frac{\exp(\sigma \cdot (l - X')) + \exp(-\sigma \cdot (l - X'))}{\exp(\sigma \cdot l) - \exp(-\sigma \cdot l)}\right]. \tag{3.9}$$

Ad. VIII. Temperature distribution in a finite transparent sample, $T(x, l, \beta \approx 0, R = 1)$.

$$T^*(x) = \frac{I_0}{\lambda \cdot \sigma^2}\,. \tag{3.10}$$

As an illustration of the application of the equation (2.13) – (2.15), for the temperature spatial distribution, the example diagrams of the distributions of the amplitude and phase of the temperature computed for the semiconductor sample of the thickness $l = 0.1$ cm, thermal diffusivity $\alpha = 0.1$ cm^2/s, optical absorption coefficient $\beta = 100$ cm^{-1}, the frequency of modulation $f = 16$ Hz and the R parameter equal 1 or -1 are presented below in Fig. 4. The characteristics presented below are typical for almost all semiconductor materials when excited below the energy gap of a given semiconductor in the region of so called Urbach tail region connected with the thermal broadening of the absorption band.

$$\text{Description of the } Y\text{-axis in Fig. 5.} \qquad \text{Amplitude} = |T(x')| \tag{3.11}$$

$$\text{Phase} = \frac{180}{\pi} \cdot \arg\left(T(x')\right) \qquad \text{Temperature} = \mathrm{Re}\left[T(x') \cdot \exp(i \cdot \omega \cdot t)\right]. \tag{3.12}$$

The analysis of the appropriate temperature distributions can lead to the interpretation of different effects observed in the photoacoustic measurements. These effects are the result of specific temperature distributions. They are illustrated in Fig. 5.

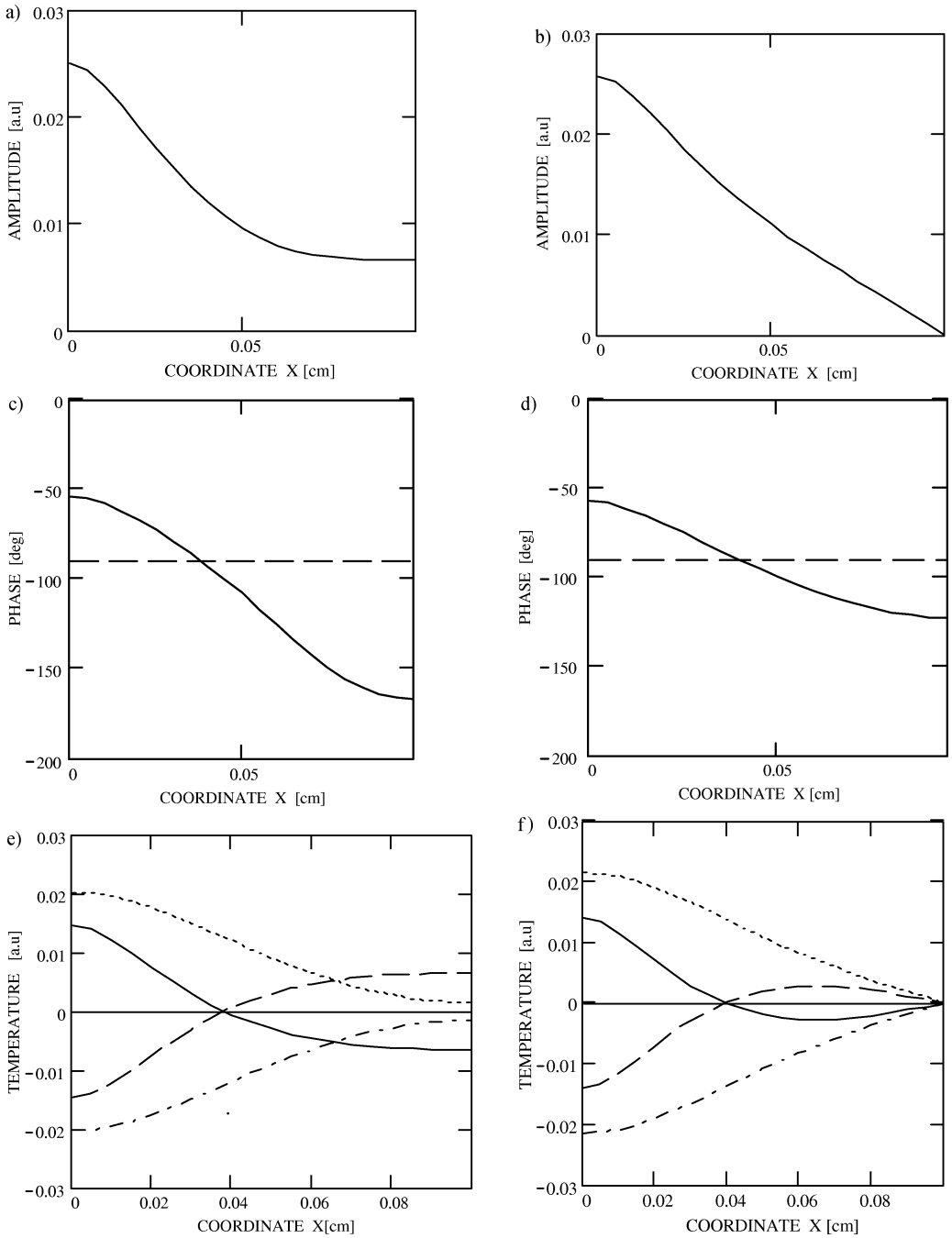

Fig. 4. Example temperature distributions in the sample for two thermal reflection coefficients values $R = 1$ (insulating backing) and $R = -1$ (thermally conducting backing). Amplitude a) and phase c) distributions of the temperature in the sample when $R = 1$. Amplitude b) and phase d) distributions of the temperature in the sample when $R = -1$. e) Instantaneous temperature distribution in the sample for $t = 0$ (solid), $t = T/4$ (dot), $t = T/2$ (dash), $t = 3T/4$ (dash-dot) and $R = 1$. f) Instantaneous temperature distribution in the sample for the same moments of time as in point e) but for $R = -1$. T – is the period of modulation of light corresponding the $f = 16$ Hz.

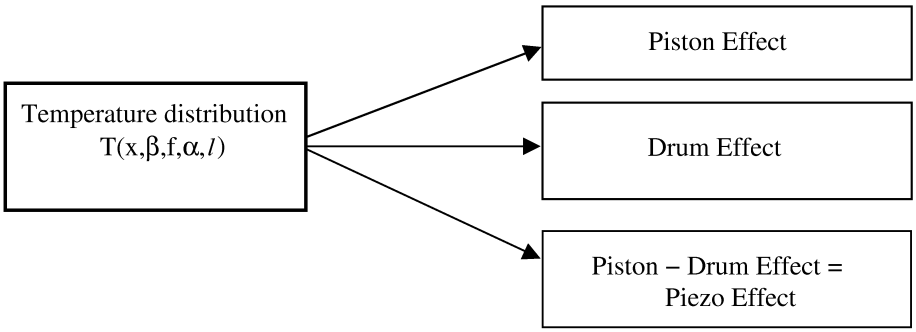

Fig. 5. Photoacoustic effects being the result of specific temperature distributions.

4. Piezo-photoacoustic spectra

The formula describing the temperature distribution in the sample $T(x)$ is important because the value of the piezoelectric photoacoustic signal is determined by this temperature distribution. Two main parts of the JACKSON and AMER [19] and BLONSKIJ [20] equations contain the temperature distribution formulae. The $S1$ function (4.1) describes that part of the piezoelectric signal that is connected with the linear thermal expansion of the sample. The $S2$ function (4.1) describes that part of the piezoelectric signal that is connected with thermoelastic bending of the sample.

$$S1 \cong \int_0^l T(x)\,dx \qquad S2 \cong \int_0^l (l/2 - x) \cdot T(x)\,dx. \tag{4.1}$$

The total piezoelectric signal called the full-drum effect being the superposition of the piston $S1$ and drum $S2$ contributions can be expressed by the following formula being so called modified Jackson & Amer equation.

$$S = -\left(\frac{1}{l} \cdot \int_0^l T(x) \cdot dx - \frac{1}{2 \cdot r^2} \cdot \int_0^l \left(\frac{l}{2} - x\right) \cdot T(x) \cdot dx\right), \tag{4.2}$$

where $r = l/2\sqrt{3}$

The sign minus (or plus) in front of the equation (4.2) depends on the way of connecting of the piezoelectric transducer to the measuring equipment.

The amplitude and phase characteristics of the piezoelectric photoacoustic signal contributions, $S1$ and $S2$, versus the optical absorption coefficient presented in Fig. 6 and the full drum S effect amplitude and phase characteristics presented in Fig. 7 were computed for the following parameters: $\alpha = 0.08$ cm^2/s, $f = 36$ Hz, $l = 0.08$ cm, $R = 1$, -1 and the temperature distribution formula given by equations (2.13) – (2.15).

The piezoelectric photoacoustic amplitude spectrum presented in Fig. 7a) exhibits three characteristic features that can be observed in most experimental piezoelectric photoacoustic spectra met in the literature of piezoelectric photoacoustic spectroscopy.

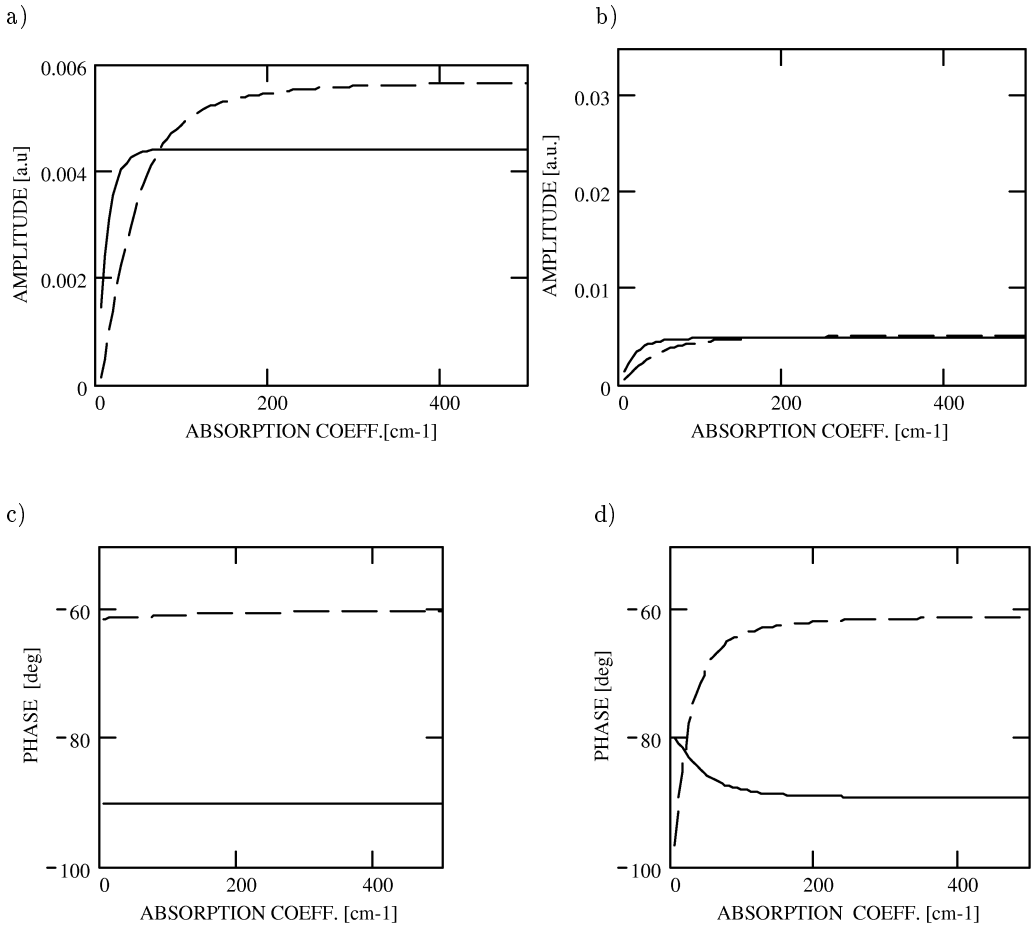

Fig. 6. Amplitude versus the optical absorption coefficient for the piston signal $S1$ (solid line) and the drum signal $S2$ (dash line) for R = 1 (a) and for R = −1 (b). Phase versus the optical absorption coefficient for the piston signal $S1$ (solid line) and the drum signal $S2$ (dash line) for R = 1 (c) and for R = −1 (d).

They are the following: a peak appearing in the region of small optical absorption followed by a dip and next the saturation region for the high values of the optical absorption coefficient.

The origin of these characteristic features can be observed in Fig. 6a). They are, in general, the result of the crossing of the piston $S1$ and drum $S2$ spectral characteristics. For low optical absorption coefficients the piston contribution $S1$ is always bigger than the drum contribution $S2$. As the total piezoelectric signal S is proportional to the difference $S1 - S2$ then the characteristic peak appears in this optical absorption region. The dip observed in Fig. 7a) is the result of the intersection of $S1$ and $S2$ spectral characteristics. The depth of the dip depends only on the phase of the drum $S2$ signal as the phase of the piston $S1$ signal is practically always −90 deg. The computer simulations indicated

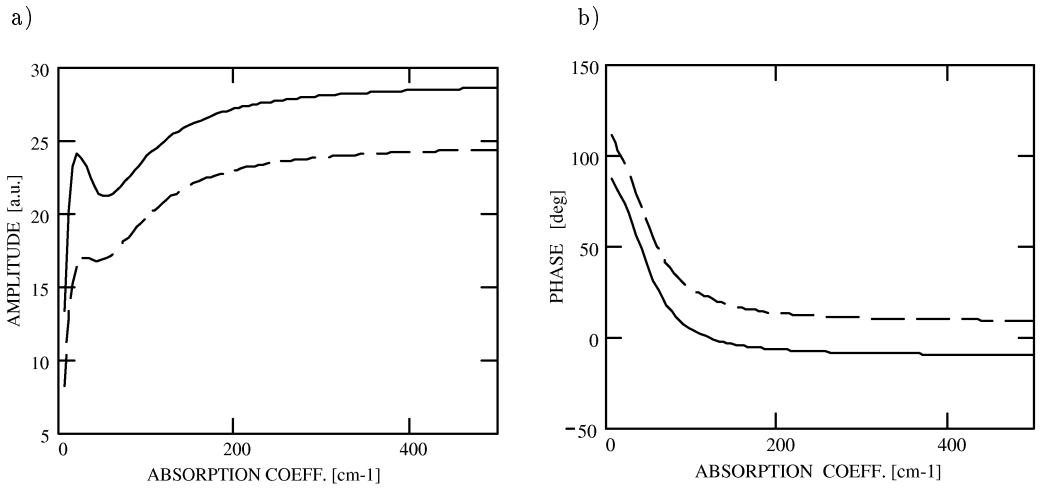

Fig. 7. a) Amplitude versus the optical absorption coefficient of the full drum (piezo effect) S for $R = 1$ (solid line) and $R = -1$ (dash line). b) Phase versus the optical absorption coefficient of the full drum (piezo effect) S for $R = 1$ (solid line) and $R = -1$ (dash line).

that with the increase of the frequency of modulation the phase of the drum $S2$ signal shifts from -30 deg to -90 deg and the dip becomes deeper.

For the higher values of the optical absorption coefficients both the piston and drum $S1$ and $S2$ signals exhibit the saturation effect i.e. their values do not depend on the value of the optical absorption coefficient and the drum contribution $S2$ is greater than the piston contribution $S1$.

4. Conclusions

This paper presents the derivation of the formula for the spatial distribution of the periodical contribution of the temperature generated in the sample excited by the in intensity modulated beam of light. The presented formula describes the temperature distribution in the sample placed on thermally and optically thick backing material. The backing material is described by the thermal reflection coefficient R. The influence of the thermal properties of the backing material ($R = 1$, $R = -1$) on the amplitude, phase and instantaneous temperature distributions is shown and discussed. The origin of the characteristic features observed in the experimental piezoelectric photoacoustic spectra is explained with the derived temperature distribution formula as a result of the difference of the piston and drum spectral characteristics. The comparison of the presented temperature distribution with other specific distributions known from the literature is shown and discussed. The presented formula enables the computations of the piezoelectric photoacoustic spectra obtained for samples placed on different backing materials.

References

[1] T. Ikari, H. Yokoyama, S. Shigetomi and F. Futagami, *Near band edge photoacoustic spectra of* p-Si *single crystals*, Jap. J. of Appl. Phys., **29**, 5, 887–890 (1990).

[2] K. Higashi, T. Ikari, H. Yukoyama and K. Futagami, *Effect of thermal donor formation on the photoacoustic spectra of* n-Si *single crystals*, Jpn. J. Appl. Phys., **32**, 2570–2572 (1993).

[3] S. Shigetomi, T. Ikari, Y. Koga and S. Shigetomi, *Annealing behavior of photoacoustic spectra of undoped InSe*, Phys. Stat. Sol. (a), **90**, K.61–K64 (1985).

[4] T. Ikari, A. Fukuyama, K. Maeda, K. Futagami, S. Shigetomi and Y. Akashi, *Photoacoustic signals of n-type* GaAs *layers grown by molecular-beam epitaxy on semi-insulating substrates*, Phys. Rev. B, **46**, 16, 10173–10178 (1992).

[5] T. Ikari, K. Miyazaki, A. Fukuyama, H. Yokoyama, K. Maeda and K. Futugami, *Piezoelectric detection of the photoacoustic signals of n-type* GaAs *single crystals*, J. Appl. Phys., **71**, 5, 2408–2413 (1992).

[6] F. Firszt, S. Łęgowski, H. Męczyńska, J. Szatkowski and J. Zakrzewski, *Photoacoustic study of* $Zn_{1-x}Be_xTe$ *mixed crystals*, Anal. Sciences, **17**, 129–132 (2001).

[7] H. Męczyńska, J. Zakrzewski, S. Łęgowski, M. Popielarski, F. Firszt, J. Szatkowski, R. Klugiewicz and K. Łęgowski, *A photoacoustic study of* $Zn_{1-x}Mg_xSe$ *mixed crystals*, Acta Physica Polonica A, **87**, 2, 547–550 (1995).

[8] J. Zakrzewski, F. Firszt, S. Łęgowski, H. Męczyńska, B. Sekulska, J. Szatkowski and W. Paszkowicz, *Photoacoustic investigations of beryllium containing wide gap II-VI mixed crystals*, Proc. 5^{th} Therminic Workshop Rome, 241–245 (1999).

[9] A. Rosencwaig and A. Gersho, *Theory of the photoacoustic effect with solids*, J. Appl. Phys., **47**, 1, 64–69 (1976).

[10] C.A. Bennett and R.R. Patty, *Thermal wave interferometry: a potential application of the photoacoustic effect*, Appl. Optics, **21**, 1, 49–54 (1982).

[11] P. Charpentier and F. Lepoutre, *Photoacoustic measurements of thermal diffusivity description of the drum effect*, J. Appl. Phys., **53**, 1, 608–614 (1982).

[12] N.F. Leite, N. Cella and H. Vargas, *Photoacoustic measurement of thermal diffusivity of polymer foils*, J. Appl. Phys., **61**, 8, 3025–3027 (1987).

[13] M. Maliński and L. Bychto, *Photoacoustic determination of thermal parameters of layers in front and rear surface illumination methods*, Molec. & Quantum Acoustcs, **18**, 169–177 (1997).

[14] M. Maliński and L. Bychto, *Photoacoustic methods of determination of thermal parameters of electronics materials*, Proc. 3^{rd} Therminic Workshop Cannes, 254–259 (1997).

[15] Z. Suszyński, M. Maliński and L. Bychto, *Thermal parameters measurement method of electronics materials*, IEEE Trans. Part A, **21**, 3, 424–434 (1998).

[16] M. Ouzafe, P.P. Poulet and J. Chambron, *Photoacoustic detection of triplet state and singlet oxygen in highly absorbing samples*, Photochem. Photobiol, **55**, 491–503 (1992).

[17] M. Maliński, L. Bychto, F. Firszt, J. Szatkowski and J. Zakrzewski, *Determination of the optical absorption coefficient of* $Zn_{1-x-y}Be_xMg_ySe$ *mixed crystals from the PAS experiments-improved approach*, Anal. Science, **17**, 133–136 (2001).

[18] M. Maliński, L. Bychto, S. Łęgowski, J. Szatkowski and J. Zakrzewski, *Photoacoustic studies of* $Zn_{1-x}Be_xSe$ *mixed crystals: two layer approach*, Microel. Journal, **32**, 10–11, 903–910 (2001).

[19] W. Jackson and N.M. Amer, *Piezoelectric potoacoustic detection: Theory and experiment*, J. Appl. Phys., **51**, 6, 3343–3353 (1980)..

[20] I.V. Blonskij, V.A. Tkhoryk and M.L. Shendeleva, *Thermal diffusivity of solids detemination by photoacoustic piezoelectric technique*, J. Appl. Phys., **79**, 7, 3512–3516 (1996).